Voltage clamp of the cardiac sodium current at 37°C in physiologic solutions

Katherine T. Murray,* Takafumi Anno, Paul B. Bennett, and Luc M. Hondeghem
Stahlman Cardiovascular Research Program, Departments of Medicine and Pharmacology, Vanderbilt University School of Medicine, Nashville, Tennessee 37232

ABSTRACT The cardiac sodium current was studied in guinea pig ventricular myocytes using the cell-attached patch voltage clamp at 37°C in the presence of 145 mM external sodium concentration. When using large patch pipettes (access resistance, 1–2 MΩ), the capacity current transient duration was typically 70 μs for voltage clamp steps up to 150 mV. At 37°C the maximum inward sodium current peaked in ~200 μs after the onset of a clamp step and at this strong depolarization, less than 10% of the sodium current developed during the capacity transient. The sodium current developed smoothly and the descending limb of the current-voltage relationship usually spanned a range of 40 mV. Moreover, currents reduced by inactivation of sodium channels could be scaled to superimpose on the maximum current. Current tails elicited by deactivation followed a monoexponential time course that was very similar for currents of different sizes. Data obtained over a range of temperatures (15°–35°C) showed that the steady-state inactivation and conductance-voltage curves were shifted to more negative voltages at lower temperatures. These results demonstrate the feasibility of investigating the sodium current of mammalian cardiac cells at 37°C in normal physiological solutions.

INTRODUCTION

Sodium channels are fundamental units of excitation and conduction in cardiac tissue. However, voltage clamp analysis of the cardiac sodium current (I_{Na}) has previously not been possible at physiologic temperatures (37°C). Under conditions where experimental temperature exceeds 25°C, the size of I_{Na} increases and the kinetics of current activation become so rapid that successful voltage clamp control has not been achieved (Johnson and Lieberman, 1971; Beeler and McGuigan, 1978; Fozzard and Beeler, 1975). In such circumstances, sodium channels become activated during charging of the membrane capacitance at a time when the membrane is not voltage clamped. Although single cells provide a much smaller membrane capacitance than multicellular preparations, the problem nonetheless persists (Makielski et al., 1987; Johns et al., 1989). For these reasons, it has only been possible to study I_{Na} of single cells at cooler temperatures (≤25°C), usually with a reduction in the sodium gradient (Brown et al., 1981). In the past, the maximum rate of rise of the action potential upstroke ($\dot{V}_{max}$) has been used as an index of I_{Na} at temperatures >25°C. However it is now apparent that at least under some conditions, these two measurements are not linearly related (Cohen et al., 1984; Sheets et al., 1988; Johns et al., 1989).

The importance of measuring the cardiac sodium current under conditions similar to those encountered in vivo is highlighted by the fact that the actions of antiarrhythmic agents may be markedly altered by changes in temperature (Johns et al., 1989) and sodium gradient (Cahalan et al., 1980). For example, as previously reported by our laboratory, *O*-desmethyl encainide is a potent blocker of activated cardiac sodium channels; however at experimental temperatures of 15–20°C, no diastolic recovery from block can be detected. At higher temperatures (35°C) using $\dot{V}_{max}$ as an approximate measure of I_{Na}, recovery from block can be demonstrated and use-dependent unblocking increases. Clearly, the results at 35°C more accurately represent the findings in vivo. In addition, rates of cellular biochemical reactions and enzymatic activity are reduced at cooler temperatures. Because metabolic regulation of ionic channel function is well described (Browning et al., 1985; Forn, 1984; Levitan, 1985; Ono et al., 1989; Schubert et al., 1989), it is again preferable to study ionic currents including I_{Na} at physiologic temperatures. Given these considerations, we set out to determine whether voltage clamp of the cardiac sodium current could be achieved at physiologic temperatures using the cell-attached patch method. Specifically, we tested whether reduction of the capacitive load by using large cell-attached patches coupled with a low access resistance would make it possible to voltage clamp

*Dr. Murray is a Charles E. Culpeper Foundation Medical Scholar.
Address correspondence to Katherine T. Murray, Division of Clinical Pharmacology, Room 560, Medical Research Building, Vanderbilt University School of Medicine, Nashville, TN 37232-6602.

0006-3495/90/03/607/7 $2.00

I_{Na} at 37°C and in sodium gradients encountered in vivo. Preliminary results of these experiments have been presented previously in abstract form (Murray and Hondeghem, 1989).

METHODS

Single adult guinea pig ventricular myocytes were prepared using collagenase dispersion. In brief, guinea pig hearts were quickly removed after cervical dislocation and perfused using a Langendorf apparatus with a cannula in the aorta. The perfusate was initially nominally calcium-free, Joklik modified minimal essential medium (Sigma Chemical Co., St. Louis, MO) for 2 min, followed by a similar solution containing collagenase 0.5 mg/ml (type III; Worthington Diagnostics Div., Freehold, NJ), trypsin 0.2 mg/ml (Gibco Laboratories, Grand Island, NY) and calcium at a concentration of 50 μM for 10 min or until a rapid drop in perfusion pressure occurred. The ventricles were cut down, minced in a modified KB medium (Isenberg and Klockner, 1982), and filtered through 210 μm teflon mesh. The cells were then centrifuged and washed twice in KB medium, resuspended in KB for 2 h, and finally incubated in modified medium 199 (Sigma Chemical Co., St. Louis, MO; 5% fetal calf serum, 24 mM $NaHCO_3$) in a 95:5% O_2/CO_2 environment until experimentation (within 12 h). Cells were placed into a small tissue bath (0.5 ml) mounted on an inverted microscope (Nikon Inc., Garden City, NJ) which was continuously perfused (0.5–1.0 ml/min) with a standard solution having the following composition (millimolars): NaCl 145, KCl 4.0, $CaCl_2$ 1.8, $MgCl_2$ 1.0, glucose 10, Hepes 10, pH = 7.35. In some experiments depolarized cells were studied using a high external potassium solution (millimolars): KCl 145, $CaCl_2$ 0.1, $MgCl_2$ 1.0, Hepes 10, glucose 10, pH = 7.35. The bath temperature was controlled using a Peltier device (Midland Ross Corp., Cambridge, MA), and variation of temperature throughout the bath was <1°C. Only quiescent rod-shaped single cells with clear cross-striations were used for experimentation, and large cells in particular were selected (see Discussion).

Micropipettes were constructed from starbore capillary tubes (Radnoti Glass Technology Inc., Monrovia, CA) and were heat polished to have tip resistances of 1–2 MΩ. The internal diameter of the pipettes was ~2 μm, and using this value, the area of the tip openings was estimated to be 3–5 μm^2 (Sakmann and Neher, 1983). Due to the density of sodium channels in these cells, electrodes of these dimensions usually resulted in maximum inward currents between 50 and 300 pA. For all experiments, pipettes were filled with the standard solution (Na_{bath} = 145 mM). To minimize pipette-bath capacitance, the electrodes were coated with Sylgard® resin (compound #184; Dow Corning Corp., Midland, MI) and submersion of the electrodes in the bath was minimized by raising the cell toward the surface. The electrodes were attached to an Axopatch voltage clamp amplifier which was driven by a 12-bit digital-to-analog converter controlled by customized pClamp software (Axon Instruments, Inc., Burlingame, CA). Electrode capacitance, series resistance, and leak currents were compensated using analog circuits. Specifically, after seal formation, fast capacity transient cancellation was used to minimize the effects of pipette capacitance on the capacity transient. Whole-cell capacity compensation was not utilized. The voltage error due to series resistance was typically very low (≤ 0.1 mV); moreover, the application of series resistance compensation frequently did not alter the appearance of the transient and therefore it was usually not needed.

Sodium currents were filtered using a four-pole Bessel filter (20 or 50 kHz: −3 dB), recorded using a 12-bit analog-to-digital converter (sampling rate = 100 kHz), and stored on magnetic disk using an IBM AT computer. Because of the relatively small number of sodium channels per patch, 8–15 individual current recordings were averaged during data collection. For data obtained using standard bath solution, membrane potentials are expressed relative to the cellular resting potential. Data are presented as mean ± 1 SD. Analysis of results at different temperatures was performed using a two-way analysis of variance.

RESULTS

The data presented at 37°C in standard solution (Na_{bath} = 145 mM) represent results of seven experiments. Cell size was 125 ± 15 μm by 29 ± 7 μm, whereas micropipette resistance in the bath solution averaged 1.4 ± 0.3 MΩ. The mean value of seal resistance was 3.0 ± 1.4 GΩ. Integration of the uncompensated capacity transient during a 20-mV depolarization that produced no sodium current indicated that the pipette-membrane capacity load ranged from 1 to 2 pF. During experiments, patch-clamped cells frequently survived longer than 1 h and occasionally up to 3 h.

As shown in Fig. 1 *A*, the capacity transients of the largest depolarizations (150 mV) were 99% complete in 70 μs in most experiments and in 100 μs in all cells. To fully remove inactivation, we held patches at 50 mV negative to the resting potential (V_R). The current-voltage (IV) relationship shown in Fig. 1 *B* was obtained by clamping to different potentials for 4 ms. Typically, I_{Na} started to develop when clamping to potentials more positive than V_R. The peak sodium current increased smoothly as the depolarizing step was further increased over the next 35–45 mV. The maximum peak I_{Na} in Fig. 1 *A* occurred near V_R + 45 mV and peaked ~210 μs after the onset of the depolarization. In all experiments, less than 10% of the sodium current had developed at the end of the capacity transient during depolarizations producing maximum peak I_{Na}. For stronger depolarizations, the current declined again and the time to peak sodium current became progressively shorter (Fig. 1 *C*). As a result, peak sodium current merged with the capacity transient for depolarizations near the reversal potential (E_{rev}). For this reason, direct measurement of E_{rev} was typically unreliable with this technique as presently employed. In this series of experiments, when using 5-mV step depolarizations (n = 6), I_{Na} was initially detected at V_R + 5 ± 4 mV, whereas peak I_{Na} occurred at V_R + 43 ± 3 mV.

Sodium currents elicited from various holding potentials are shown in Fig. 2 *A*. The time to peak I_{Na} for currents of different sizes was constant. Moreover, each of the smaller currents in the family could be scaled to superimpose upon the largest sweep. The resulting steady-state inactivation curve is displayed in Fig. 2 *B*. When data were fit with the Boltzmann equation, the midpoint of the curve ($V_{1/2}$) for these experiments aver-

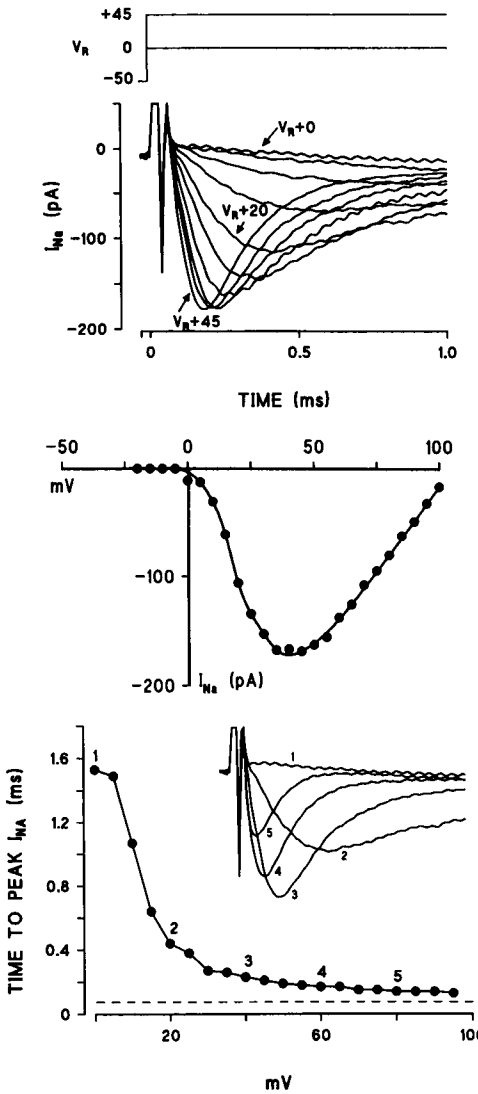

FIGURE 1 (*A*) The sodium currents produced by progressive 5 mV step depolarizations 4 ms in duration are shown without subtraction of the capacity transient. The voltage clamp protocol showing two steps is displayed above the currents. V_R represents the resting potential of the cell. The data were filtered digitally at 10 kHz after collection for analysis. (*B*) The peak current-voltage relationship corresponding to the records in *A* is shown. Voltage steps are expressed as mV change relative to the resting membrane potential. (*C*) The time to peak sodium current for the cell in *A* is plotted as a function of the voltage step expressed as mV change relative to the resting membrane potential. The inset shows the corresponding current traces for every fourth point or voltage step. The dashed line represents a value of 70 μs, which defines the completion of the capacity transient in this experiment.

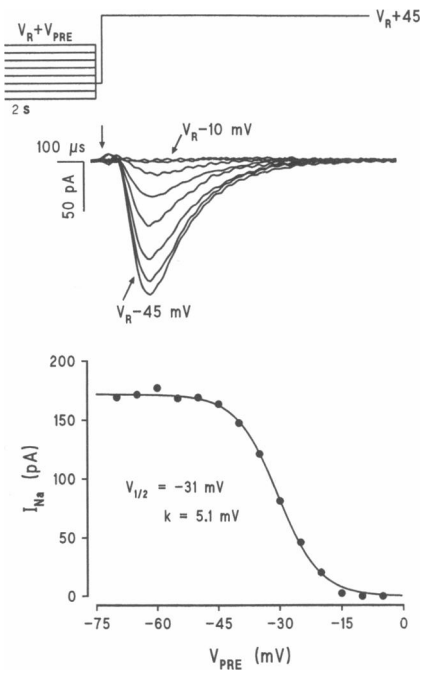

FIGURE 2 (*A*) Sodium currents elicited from various holding potentials are illustrated (same cell as Fig. 1). The data were digitally filtered at 20 kHz after collection. The capacity transient was subtracted using an average of several sweeps without sodium current. Progressive 5 mV step conditioning depolarizations were 2 s in duration and are expressed as the resting membrane potential (V_R) plus a prepulse conditioning voltage (V_{PRE}). The test pulse was V_R + 45 mV. The voltage clamp protocol is shown above the current traces. (*B*) The steady-state inactivation curve corresponding to the currents displayed in *A* is plotted. Voltage steps are expressed as the prepulse conditioning voltage (V_{PRE}) shown in Fig. 2 *A*. The solid curve describes the least squares fit of the data with the Boltzmann equation for distribution of the sodium channel between the available and unavailable states. The voltage at which 50% of the channels were available to open ($V_{1/2}$) was V_R − 31 mV with a slope factor (k) of 5.1 mV.

aged V_R − 30 ± 11 mV, with a mean slope factor (k) of 4.8 ± 0.8 mV. For individual experiments at 37°C, the preparation was quite stable: the amplitude of I_{Na} did not change, nor did the voltage dependence of inactivation drift as a function of time after seal formation (Kunze et al., 1985; Makielski et al., 1987). The maximum shift observed in the steady-state inactivation curve was only 5 mV with stabilization after 30 min.

Fig. 3 demonstrates deactivating tail currents generated by stepping from 50 mV negative to V_R to the voltage that yielded the maximum sodium current (V_R + 45 mV), and then back to V_R at different times after activation of the current. Each deactivating current tail exhibited a smooth monoexponential decline of similar time course (τ = 61 ± 3 μs), indicating successful voltage clamp of the peak current observed.

The effect of temperature upon I_{Na} kinetics was investigated in 10 additional cells. The typical changes that occurred upon warming the bath in a single cell are displayed in Fig. 4 (Na_{bath} = 145 mM; n = 3). When compared with the IV relationship obtained at 35°C, the

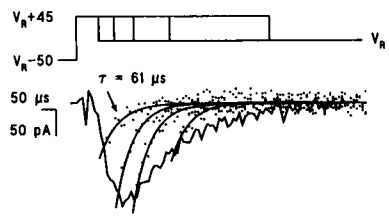

FIGURE 3 Deactivation tail currents were generated by stepping from the resting potential (V_R) −50 mV to a level producing maximal sodium current (V_R + 45 mV) and back to V_R. The voltage clamp protocol is shown above the current records. The raw data are plotted as individual points. The corresponding fitted curves are superimposed as solid lines and demonstrated a smooth monoexponential decline having an average time constant of 61 ± 3 μs.

size of the current was progressively reduced at colder temperatures (Fig. 4 *A*). Although E_{rev} was not measured directly, an estimate could be obtained by extrapolation along with the linear positive slope of the IV curve, and this value was used to construct the corresponding conductance (g_{Na})-voltage plots shown in Fig. 4 *B*. Normalized curves for steady-state inactivation and relative conductance are displayed in Fig. 4 *C*; both demonstrated a shift to the left at lower temperatures. To explore further the voltage sensitivity of temperature-dependent sodium channel gating, data were also obtained in depolarized cells having a resting potential near 0 mV (K_{bath} = 145 mM; n = 7). Under such conditions, similar results were obtained with a shift of the steady-state inactivation curve to more negative voltages with lower temperatures (Table 1). There was a trend toward reduction in the slope factor as well. For the IV relationship, no significant change occurred in the voltage producing maximal inward current (16°C = −29 ± 9 mV; 26°C = −27 ± 5 mV; 36°C = −27 ± 6 mV). In experiments where peak I_{Na} was >50 pA at all temperatures, relative g_{Na} were curves constructed using estimated E_{rev}. These curves also showed a similar shift to more negative voltages at cooler temperatures: for 16°C (n = 3), $V_{1/2}$ = −57 ± 10 mV, k = −7.9 ± 1.8 mV; for 26°C (n = 3), $V_{1/2}$ = −49 ± 6 mV, k = −9.2 ± 0.2 mV; for 36°C (n = 2), $V_{1/2}$ = −44 mV, k = −8.8 mV. Estimated E_{rev} for experiments at 36°C in depolarized cells was 54 ± 3 mV (n = 3).

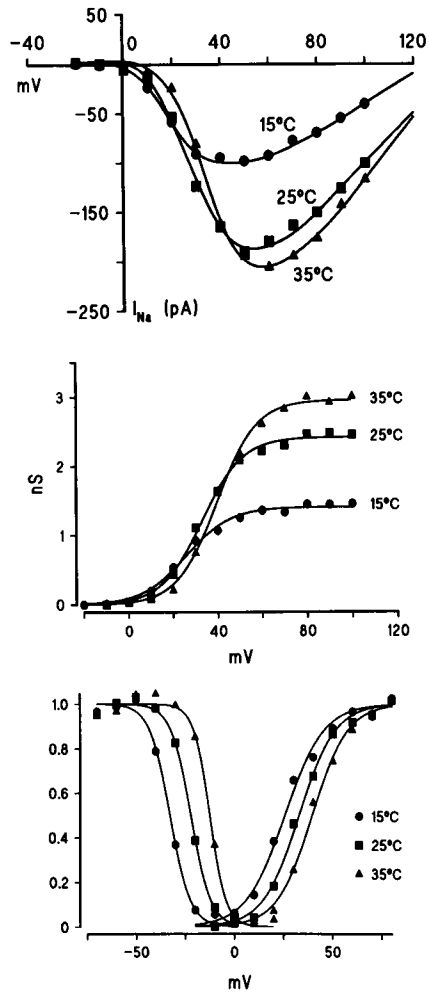

FIGURE 4 (*A*) The peak current-voltage relationship is shown in a given cell over a range of experimental temperatures (15–35°C) in standard solution Na_{bath} = 145 mM). Voltage steps are expressed as mV change relative to the resting membrane potential. Curves were drawn through the data points using a spline fit. At colder temperatures, peak I_{Na} decreased in magnitude. (*B*) Conductance (g_{Na})-voltage plots that correspond to the IV relationships in Fig. 4 *A* are shown with g_{Na} displayed on the ordinate. The solid lines represent the least squares fit of the data with the Boltzmann equation. (*C*) Normalized curves for steady-state inactivation (*on the left*) and relative conductance (*right*) are illustrated for the same cell as in Fig. 4 *A*. The fitted curves were constructed using the Boltzmann equation. At colder temperatures, both the h- and g_{Na}-curves were shifted to more negative voltages.

DISCUSSION

Our results demonstrate for the first time that the cardiac sodium current can be voltage clamped at 37°C in physiologic solutions using the large cell-attached patch technique. The sodium current under these conditions should more closely represent sodium channel current in vivo, especially because measurements are made using intact cells with preservation of their internal milieu. In the whole-cell voltage clamp technique, the cell interior dialyzed with the pipette solution and the voltage dependence of the macroscopic inactivation and activation drift

TABLE 1 **Steady-state inactivation of I_{Na} in depolarized cells**

	16°C (n = 7)		26°C (n = 7)		36°C (n = 3)	
	$V_{1/2}$	k	$V_{1/2}$	k	$V_{1/2}$	k
Mean ±	−116‡	4.3*	−109‡	4.8	−98	4.9
SD	6	1.1	5	0.6	2	0.3

Data were fit with the Boltzmann equation using $V_{1/2}$ = midpoint (mV), k = slope factor (mV).
*$P < 0.05$ compared with value at 36°C.
‡$P < 0.01$ compared with value at 36°C.

to more negative potentials (Makielski et al., 1987). The cell-attached patch yielded a more stable preparation that exhibited little or no apparent drift of voltage dependence as a function of time at a constant temperature.

By minimizing the capacity load to be charged as well as the access resistance, voltage clamp can be achieved in 70–100 μs in such patches. As a result, the sodium current was separated from the capacity transient at most potentials, even at 37°C. In this preparation, the sodium current appeared to be well controlled because: (*a*) the currents were smooth in contour and devoid of "abominable notches" (Cole and Moore, 1960; Cole, 1968) and the descending limb of the current-voltage relation developed over a 40-mV range; (*b*) currents that had been reduced by inactivating sodium channels had constant time to peak values and could be scaled to superimpose; and (*c*) deactivation of sodium currents of different sizes yielded smoothly declining tail currents which could be approximated by a single exponential process (Colatsky and Tsien, 1979). Measurement of macroscopic sodium currents from cell-attached patches has been reported by other investigators (Zilberter et al., 1982; Pusch et al., 1989), but its utility in achieving voltage control at higher temperatures has not been previously investigated. Adequate voltage control using this technique resulted from use of a relatively large electrode to study a small area of cellular membrane. The large electrode reduced the access resistance to the patch, whereas the small patch minimized the membrane capacitance to be charged but nevertheless contained enough sodium channels to generate a macroscopic sodium current. The majority of the capacitive load in this situation actually arose from the distributed pipette capacitance rather than the cell membrane. Patch pipettes with tip resistances of 1–2 MΩ were ideal for such experiments in guinea pig myocytes. The estimated tip opening of our pipettes was 3–5 μm^2. However, as the membrane within a pipette typically assumes an Ω-shaped configuration with application of suction (Sakmann and Neher, 1983), the actual area of the patch under study was probably considerably larger than this value. The size of the patch can be estimated as the surface area of a hemisphere having a diameter somewhat larger than the pipette internal tip diameter. If one assumes a diameter of 6–7 μm, for example, this would give an area of 57–67 μm^2 with an estimated $\dot{V}_{max}$ of 260–360 V/s, which is consistent with values observed in single cardiac ventricular myocytes (Salata and Wasserstrom, 1988; Johns et al., 1989). It should be emphasized that estimating patch size in this way is quite empiric and depends on a number of assumptions. In cells with greater density of channels, a smaller pipette may be desired (and vice versa).

In these experiments, we selected large cells to minimize depolarization of the cell by the inward current in the patch. However, the question arises whether the membrane potential of the cell indeed remained constant during the flow of sodium current through the patch. Using the model of a right circular cylinder for guinea pig myocytes, mean cell surface area was calculated to be 11,300 μm^2. This corresponds to an average cell membrane capacitance of 113 pF. Integration of the largest I_{Na} for the cell shown in Fig. 1 *A* resulted in a total charge transfer through the patch of 43×10^{-15} Coulombs causing a depolarization of < 0.4 mV. Therefore, even for much larger currents, depolarization of the cell should always be < 1 mV, such that current passed through the patch would not affect the voltage clamp significantly.

Our results demonstrate that the voltage sensitivity of sodium channel gating was variable over a broad range of experimental temperatures. In a "physiologic" solution (Na_{bath} = 145 mM), both steady-state inactivation and relative conductance-voltage curves shifted to more negative voltages at colder temperatures. Similar results were obtained in cells with known resting membrane potentials, i.e., those depolarized to 0 mV (K_{bath} = 145 mM). This latter finding eliminated the possibility that changes in resting membrane potential were responsible for the observed shifts. The reason(s) for such shifts in sodium channel gating is unclear, but possibilities include a membrane phase transition which could modify membrane lipids and their interations with the sodium channel protein, as suggested for frog and rabbit muscle membrane (Kirsch and Sykes, 1987); changes in the electric field sensed by the sodium channel protein due to charge transfer (Hille et al., 1975) as a result of changes in metabolic processes such as phosphorylation (Ono et al., 1989; Schubert et al., 1989); and variation in the heights of the energy barriers involved in sodium channel gating transitions which could alter one or more transition rate constants (Hille, 1984). Based on the information available, it is impossible to differentiate among such possibilities at the present time. Interestingly, a different response to alteration in temperature was found in mammalian nerve (Schwartz, 1986) than that seen by us in cardiac

ventricular muscle. On warming from 0° to 22°C, the *h*-curve shifted to more positive voltages, but no further shift was observed as temperature was raised further to 37°C. The cause of this difference between the two experimental preparations is not known.

A potential disadvantage of the cell-attached patch technique is the inability to measure cellular resting potential at the time data are collected using physiologic solutions. In our experiments using a standard solution (Na_{bath} = 145 mM), an estimate of the transpatch potential based on threshold and peak values for the sodium current was −65 mV. From data obtained with depolarized cells, where the membrane potential was known, the average resting potential of the cells studied initially was estimated to be −68 mV, based on comparison of *h*-curve midpoints of the two groups of cells. Thus, the variable *h*-curve midpoint values of cells in the standard solution were probably due to differences in resting membrane potential (Figs. 2 *B* and 4 *C*). In the present study, steady-state inactivation occurred at more negative voltages than is typically reported for whole-cell I_{Na} (Bodewei et al., 1982; Kunze et al., 1985; Benndorf et al., 1985; Makielski et al., 1987). Kunze and co-workers reported in neonatal rat ventricular myocytes that inactivation was shifted to more negative potentials in ensemble currents from cell-attached and excised patches as compared with whole-cell currents (Kunze et al., 1987). Moreover, this shift occurred quickly over a few minutes with final $V_{1/2}$ of −100 mV (T = 20°C). We did not observe such a time-dependent shift following achievement of a gigaseal. However, we cannot exclude that this did occur but was too rapid at 37°C to be detected. A similar shift of the steady-state inactivation curve has also been observed in cell-attached and excised patches in canine ventricular myocytes (Berman et al., 1989). It is possible that the leftward shift of inactivation observed in such patches results from a structural change in the sodium channel protein under study at the time of patch formation. An alternative explanation is a localized interaction between the pipette glass and the cell membrane such that the electric field sensed by the channels is altered (Hille et al., 1975).

In summary, these results demonstrate that the cardiac sodium current can be adequately voltage clamped at 37°C in physiologic sodium concentrations. These conditions are necessary for a complete understanding of drug-channel interactions which are known to be altered by temperature and permeant ion concentration. The sodium current at 37°C was qualitatively similar to that at colder temperatures. A predictable and graded shift of gating kinetic parameters was observed, particularly with regard to steady-state inactivation of the channels. This differs from the temperature-dependent shift that occurs in mammalian nerve which saturates at 25°C.

This work was supported by grant HL36020 from the U.S. Public Health Service and the Charles E. Culpeper Foundation.

Received for publication 1 May 1989 and in final form 27 September 1989

REFERENCES

Beeler, G. W., and J. A. S. McGuigan. 1978. Voltage clamping of multicellular myocardial preparations: capabilities and limitations of existing methods. *Prog. Biophys. Mol. Biol.* 34:219–254.

Benndorf, K., W. Boldt, and B. Nilius. 1985. Sodium current in single myocardial mouse cells. *Pfluegers Arch. Eur. J. Physiol.* 404:190–196.

Berman, M. F., J. S. Camardo, R. B. Robinson, and S. A. Siegelbaum. 1989. Single sodium channels from canine ventricular myocytes: voltage dependence and relative rates of activation and inactivation. *J. Physiol. (Lond.).* 415:503–531.

Bodewei, R., S. Hering, B. Lemke, L. V. Rosenshtraukh, A. I. Undrovinas, and A. Wollenberger. 1982. Characterization of the fast sodium current in isolated rat myocardial cells: simulation of the clamped membrane potential. *J. Physiol. (Lond.).* 325:301–315.

Brown, A. M., K. S. Lee, and T. Powell. 1981. Sodium current in single rat heart muscle cells. *J. Physiol. (Lond.).* 318:479–500.

Browning, M. D., R. Huganir, and P. Greengard. 1985. Protein phosphorylation and neuronal function. *J. Neurochem.* 45:11–23.

Cahalan, M., B. I. Shapiro, and W. Almers. 1980. Relationship between inactivation of sodium channels and block by quaternary derivatives of local anesthetics and other compounds. *In* Molecular Mechanisms of Anesthesia. B. R. Fink, editor. Raven Press, New York. 17–33.

Cohen, C. J., B. P. Bean, and R. W. Tsien. 1984. Maximal upstroke velocity as an index of available sodium conductance: comparison of maximal upstroke velocity and voltage clamp measurements of sodium current in rabbit Purkinje fibers. *Circ Res* 54:636–651.

Colatsky, T. J., and R. W. Tsien. 1979. Sodium channels in rabbit cardiac Purkinje fibres. *Nature (Lond.).* 278:265–268.

Cole, K. S. 1968. Membranes, Ions, and Impulses: a Chapter of Classical Biophysics. University of California Press, Los Angeles. 325–353.

Cole, K. S., and J. W. Moore. 1960. Ionic current measurements in the squid giant axon membrane. *J. Gen. Physiol.* 44:123–167.

Forn, J. 1984. Integrated actions of cyclic nucleotides, calcium, and protein phosphorylation in the nervous system. *Adv. Cyclic Nucleotide Protein Phosphorylation Res.* 17:473–482.

Fozzard, H. A., and G. W. Beeler. 1975. The voltage clamp and cardiac electrophysiology. *Circ. Res.* 37:403–413.

Hille, B. 1984. Ionic Channels of Excitable Membranes. Sinauer Associates, Sunderland, MA. 159–162.

Hille, B., A. M. Woodhull, and B. I. Shaprio. 1975. Negative surface charge near sodium channels of nerve: divalent ions, monovalent ions and pH. *Phil. Trans. Roy. Soc. London Ser. B.* 270:301–318.

Isenberg, G., and U. Klockner. 1982. Calcium tolerant ventricular myocytes prepared by preincubation in a "KB medium." Pfluegers Arch. Eur. J. Physiol. 395:6–18.

Johns, J. A., T. Anno, P. B. Bennett, D. J. Snyders, and L. M. Hondeghem. 1989. Temperature and voltage dependence of sodium channel blocking and unblocking by O-demethyl encainide in isolated guinea pig myocytes. *J. Cardiovasc. Pharmacol.* 13:826–835.

Johnson, E. A., and M. Leiberman. 1971. Heart: excitation and contraction. *Annu. Rev. Physiol.* 33:479–532.

Kirsch, G. E., and J. S. Sykes. 1987. Temperature dependence of Na currents in rabbit and frog muscle membranes. *J. Gen. Physiol.* 89:239–251.

Kunze, D. L., A. E. Lacerda, D. L. Wilson, and A. M. Brown. 1985. Cardiac Na currents and the inactivating, reopening, and waiting properties of single cardiac Na channels. *J. Gen. Physiol.* 86:691–719.

Levitan, I. B. 1985. Phosphorylation of ion channels. *J. Membr. Biol.* 87:177–190.

Makielski, J. C., M. F. Sheets, D. A. Hanck, C. T. January, and H. A. Fozzard. 1987. Sodium current in voltage clamped internally perfused canine cardiac Purkinje cells. *Biophys. J.* 52:1–11.

Murray, K. T., and L. M. Hondeghem. 1989. Voltage clamp of the cardiac sodium current at 37°C: reduction by mexiletine. *Biophys. J.* 55:312a. (Abstr.).

Ono, K., T. Kiyosue, and M. Arita. 1989. Isoproterenol, DBcAMP, and forskolin inhibit cardiac sodium current. *Am. J. Physiol.* 256:C1131–C1137.

Pusch M., F. Conti, and W. Stuehmer. 1989. Intracellular magnesium blocks sodium outward currents in a voltage- and dose-dependent manner. *Biophys. J.* 55:1267–1271.

Sakmann, B., and E. Neher. 1983. Geometric parameters of pipettes and membrane patches. *In* Single-channel Recording. B. Sakmann and E. Neher, editors. Plenum Press, New York. 37–51.

Salata J. J., and J. A. Wasserstrom. 1988. Effect of quinidine on action potentials and ionic currents in isolated canine ventricular myocytes. *Circ. Res.* 62:324–337.

Schubert, B., A. M. J. VanDongen, G. E. Kirsch, and A. M. Brown. 1989. β-adrenergic inhibition of cardiac sodium channels by dual G-protein pathways. *Science (Wash. DC).* 245:516–519.

Schwarz, J. R. 1986. The effect of temperature on Na currents in rat myelinated nerve fibres. *Pfluegers Arch. Eur. J. Physiol.* 406:397–404.

Sheets, M. F., D. A. Hanck, and H. A. Fozzard. 1988. Nonlinear relation between V_{max} and I_{Na} in canine cardiac Purkinje cells. *Circ. Res.* 63:386–398.

Zilberter, Y. I., E. N. Timin, Z. A. Bendukidze, and N. A. Burnashev. 1982. Patch-voltage-clamp method for measuring fast inward current in single rat heart muscle cells. *Pfluegers Arch. Eur. J. Physiol.* 394:150–155.